MEKATRONIKA
e-ISSN: 2637-0883
VOL. 5, ISSUE 2, 50 – 56
DOI: https://doi.org/10.15282/mekatronika.v5i2.9843

ORIGINAL ARTICLE

Identification of Transfer Function to Model Brush Temperature of a Small DC Machine at No-Load

Muhammad Syawal Mat Jahak[1,*], Ismayuzri Ishak[1], Suhaimi Puteh[1], Sutiman[2] and I. Wayan Adiyasa[2]

[1]Faculty of Manufacturing and Mechatronic Engineering Technology, Universiti Malaysia Pahang Al- Sultan Abdullah, 26600 Pahang, Malaysia.
[2]Automotive Engineering Education, Faculty of Engineering, Universitas Negeri Yogyakarta, Indonesia.

ABSTRACT – Using temperature measurement to provide insight into the health condition of an electrical machine at any operating point could be possible if a baseline temperature of the machine could be modeled in real-time and compared to the actual current temperature. In this study, transfer functions are being identified to be used as a baseline temperature response model for a small dc machine. As a preliminary study, the transfer functions are identified using experimental data of temperature responses at several no-load speed step input. The order of transfer function tested was between a range from 0 to 4. The third order transfer function was found to be the best followed by the first order transfer function with a model MSE error of less than 0.41 and 0.65 respectively. The slight variation on the poles of the system indicates that the thermal system of the electrical machine does not obey exactly the LTI hypothesis.

ARTICLE HISTORY
Received: 9th Oct 2023
Revised: 25th Oct 2023
Accepted: 1st Nov 2023
Published: 13th Nov 2023

KEYWORDS
Thermal Analysis
Transfer Function
Condition Monitoring
Electrical Machine

INTRODUCTION

In machine diagnosis, having the measurement of the inter- ested parameter alone is not sufficient. Diagnosis could only be done with the condition that a reliable baseline data for the reference parameter is available. There is multiple method of diagnosis available in the market, the frequently employed being vibration and current signal analysis [1], [2]. However, these two methods incur non-negligible equipment costs and require expertise. Another method that is less explored is the thermal diagnosis. Other than thermal imaging, which only ap- plicable when obvious damage occurs, cheaper method using thermocouple is less discussed. This due to the slower thermal response time (larger time constant), therefore difficulty to detect the discrepancy in steady-state temperature [3], [4], [5]. Furthermore, this would require the line to be stopped to test the electrical machine temperature response to a step current input in industrial settings. A potential solution that would allow the usage of temperature data as diagnosis tools in real time is to have the baseline temperature of the components available in real-time, during the operation of the machine. By having a temperature measurement in parallel, the comparison between the real-time baseline temperature and the actual temperature would give insights to the health condition of the components of the machine (Figure 1). This would allow the development of further automated monitoring system that is less expensive.

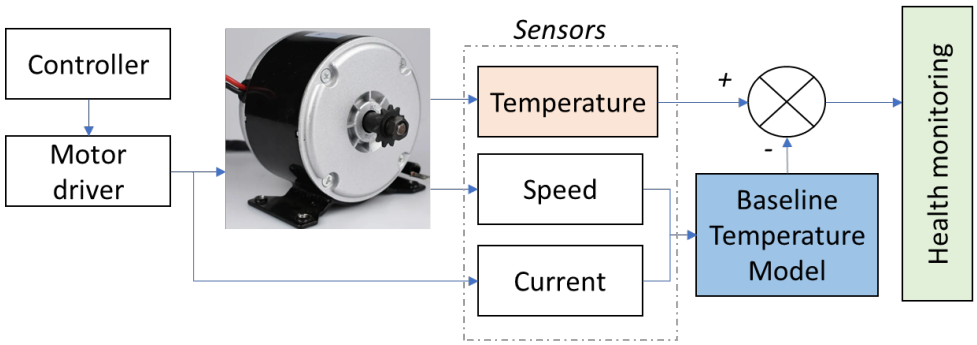

Figure 1. Real-time baseline temperature from model compared to actual temperature to provide health condition insight.

It is therefore deemed important to have a reliable thermal model that will output the baseline temperature of the machine at any operating points (speed and load). Several conditions are necessary for the thermal model. First, the model need to be precise in replicating the baseline temperature, which is the temperature of the ideal new machine without faults, wear and tear. Secondly, the model needs to be responsive and consume the least amount of computational power as possible. In the area of thermal modeling, approaches like finite element model and lumped parameter thermal network (LPTN) were explored vastly and have their respective advantages and inconveniences [6], [7] . The former being precise

*CORRESPONDING AUTHOR | Muhammad Syawal Mat Jahak | muhdsyawalmatjahak@gmail.com

© The Authors 2023. Published by Penerbit UMPSA. This is an open access article under the CC BY-NC 4.0 license.

but heavy while the later is lighter in computational requirements but requires deep understanding on heat transfer in order to be precise. When it comes to real-time applications, the LPTN is the obvious solutions as it offers the possibility of being much more responsive and computationally lighter. The LPTN is built using lumped characterized by the geometrical dimensions and material properties such as thermal conductance and specific heat. This is essential to machine designers who want to have the possibility of optimizationy by modifying these parameters. However, all the precision in the discretization of an LPTN is only necessary if the model is to be used for further parametrical optimization. From the point of view of machine health monitoring and diagnosis, this information are irrelevant. The only necessary information are the temperatures of certain components, without dealing with the details of geometric and material characteristics.

From that remarks, it is more advantageous if a lighter ther- mal model without the unnecessary information of the lumps characteristics could be developed. One potential method that could be used to create such model is by using the transfer function [8]. Transfer function is a mathematical relationship between the input and output signals of a linear, time-invariant (LTI) system that could be descirbed as in Eq. 1, where R(s) is the input of the system and C (s) is the output of the system.

$$\boldsymbol{G(s)} = \frac{C(s)}{R(s)} \tag{1}$$

It is represented as the ratio of the Laplace transform of the output signal to the Laplace transform of the input signal in the frequency domain. The step response could be used to char- acterize the thermal system of the electrical machines, giving a transfer function representative of the machine thermally. The typical temperature response of an electrical machine could be qualified as a first order response, where the transient temperature rises then settles at a steady state value when the thermal equilibrium is achieved [6] . This could be represented by Eq. 2 and illustrated by Fig. 2.

$$\Delta \mathrm{T} = Q_{th} R_{th} \left(1 - e^{-t/\tau}\right) \tag{2}$$

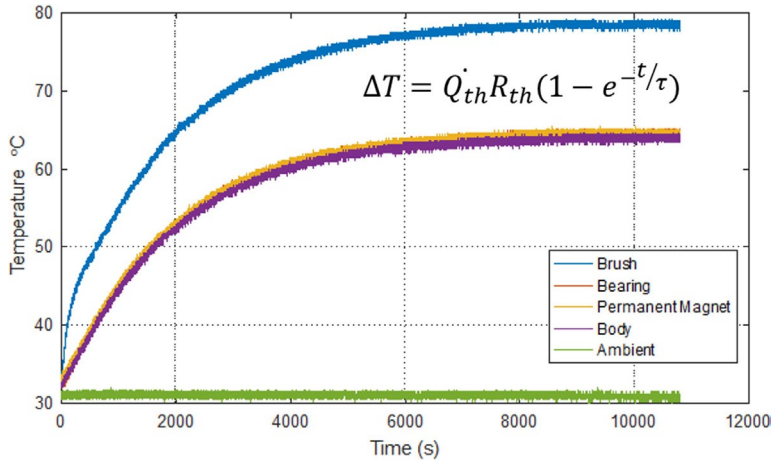

Figure 2. Typical temperature response of an electrical machine to a step losses input.

The input of the system could be multiple, which are parameters of control that may change the temperature of the machine as response, including the current (which is the image of the load) and the speed (which may affect the convection inside the machine).

METHODOLOGY

The motor used in this study is a 250W brushed dc motor with the common model name of MY1016. The specification of the motor is shown in Table I. It is instrumented with thermocouples type-K placed on several parts of the motor, including the casing, bearing, permanent magnet, brush, and ambient air as shown in Figure 3. The overall test bench can be seen in Figure 4. The temperature data acquisition by its data logger is monitored in real-time via a host PC.

Table 1. Specification of the My1016 Brushed DC Motor.

Parameter	Values
Operating Voltage	24 V
Rated current	13.5 A
Rated speed	2650 rpm
Rated torque	100 N.cm
Operating power/output	250 W
No-load Current	< 2.2 A
Shaft diameter	12.2 mm
Weight	2.3 kg

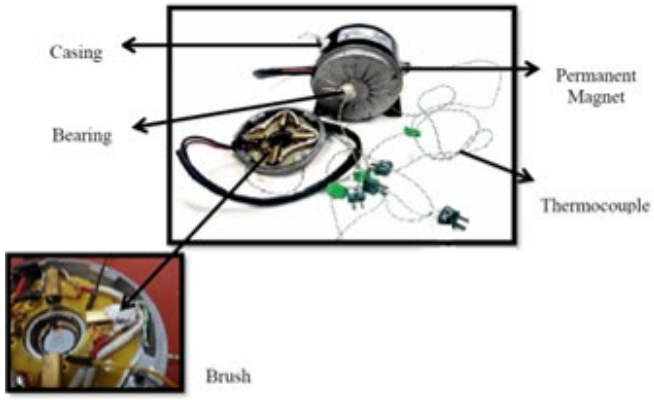

Figure 3. Thermocouples instrumented on the MY1016 dc machine.

After having verified that the no-load current of the machine at different speed through the speed range of 0 to 2650rpm at around 4mA which is considered negligible, the transfer function will be therefore developed to account for different temperature generated at different speed at no-load. The study is divided into 2 main parts: Temperature step response data generation and identification of transfer function that can be described as in Fig. 5.

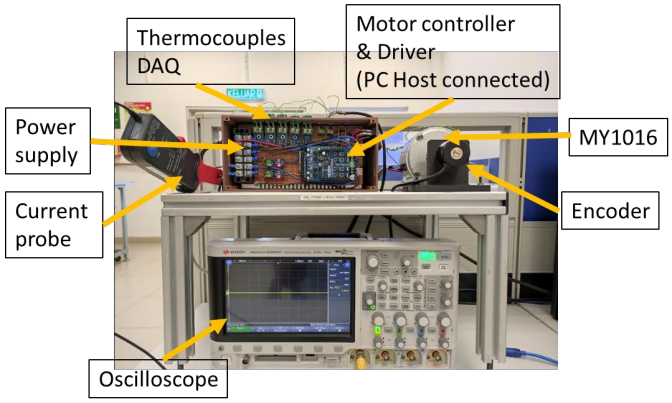

Figure 4. The complete experimental setup.

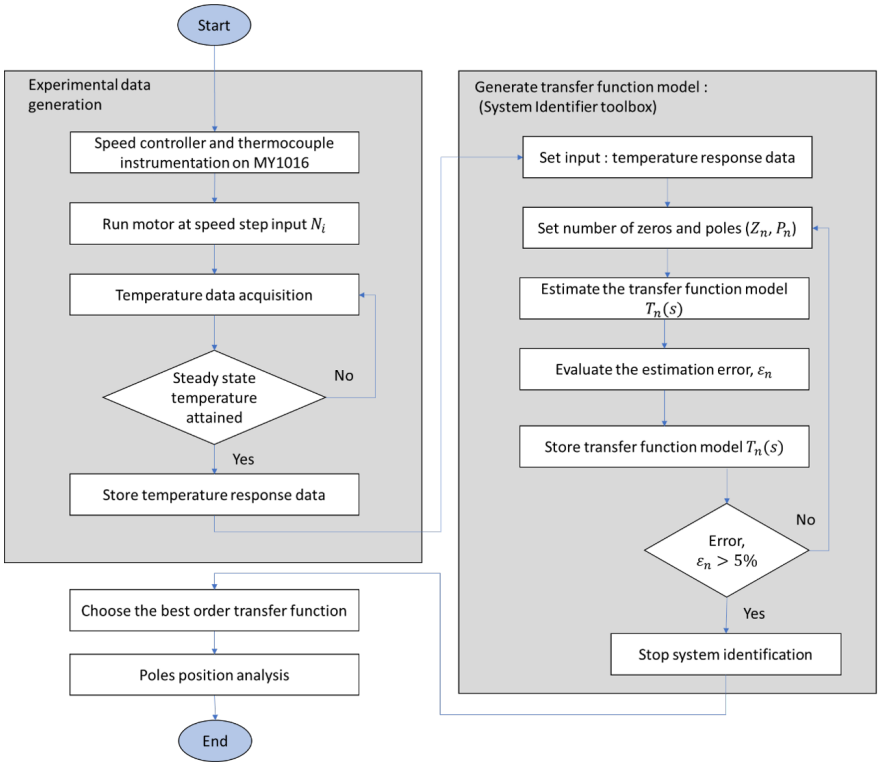

Figure 5. Flow chart of the development of transfer function for temperature response of the MY1016 dc machine.

The temperature response to a speed step input were col- lected at 5 different speeds, with each a ratio of the nominal speed (20% up to 100%). The temperature was recorded up to steady state temperature, for all the following components: brush, bearing, permanent magnet , and casing. After that, the temperature response data were used to identify a transfer function that would model it. The 'System Identification' toolbox of Matlab was here deployed (Figure 6).

By inputting the experimental data of both the speed step input and the temperature response, the tool allow us to find the corresponding transfer function with the condition of setting the number of zeros and poles of the transfer function. The generic form of a transfer functions considering its poles is as shown in Equation 3.

$$G(s) = \frac{1}{a_n s^n + a_{(n-1)} s^{(n-1)} + \cdots + a_0} \tag{3}$$

With n the order of the system, a a real number, and the values of s solving the polynomials in the denominator are the poles.

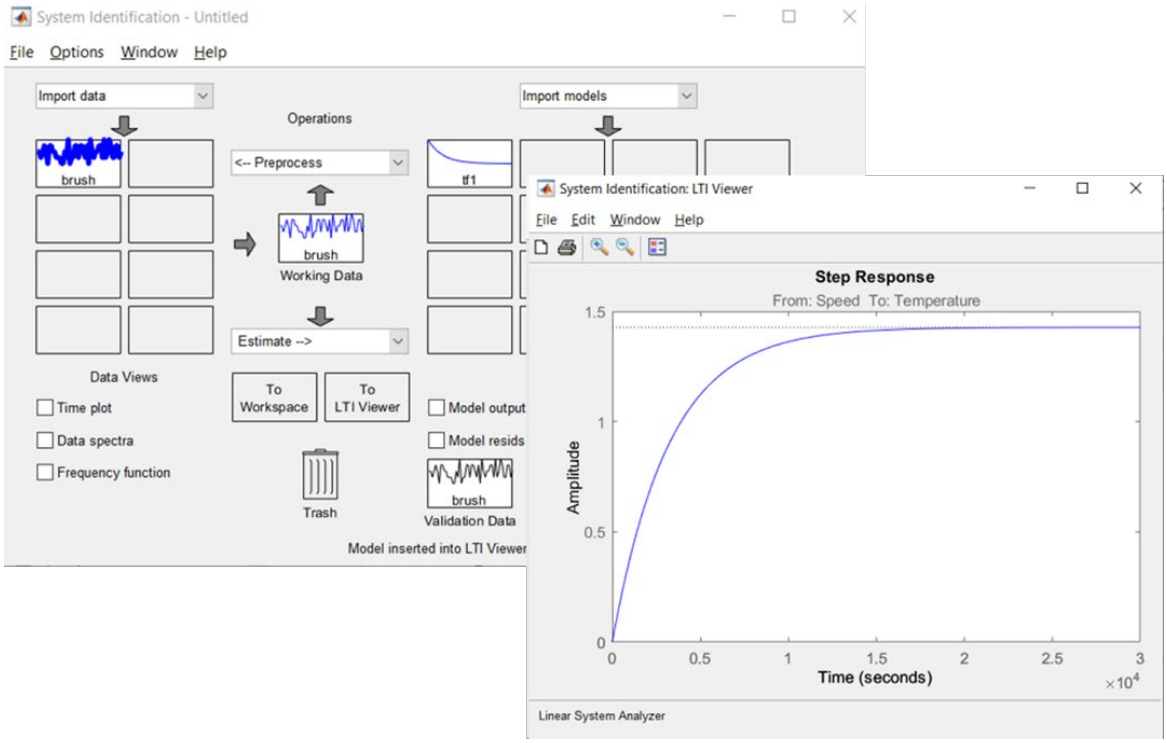

Figure 6. The system identification toolbox and its process flow.

No zeros were chosen, while for poles, different values were tested from single pole to 4 poles (this represents system of first order to fourth order). A temperature response could not be physically considered as second order system as there is no possibility of temperature oscillations like in mechanical or electrical system. However, for the purpose of only having a precise mathematical model that is not necessarily attached to a physical reality, it could be considered as higher than first order with a high damping value (overdamped system). This is especially convenient for a model that is going to be used just to monitor the baseline temperature at high precision, not considering the possibility for usage in optimization model purpose.

Following the transfer function identification process, the model error in comparison to experimental data will be eval- uated in terms of its mean-squared error (MSE) value. The transfer function that has the lowest MSE would be chosen to represent the components' temperature response to different speed at no load

RESULTS AND DISCUSSIONS

In this section, we will first present and discuss the tem- perature response data gathered from speed step input of all components at different speed before mentioned. Then the result of transfer function identification with its error will be thoroughly discussed.

Temperature response experimental data

The temperature responses were recorded up to steady state temperature, which takes 10,000 seconds for all components. Figure 7 shows a sample of temperature response data that was taken at 40% of the nominal speed. It shows that the brush has the highest temperature, followed by the bearing, permanent magnet and casing. The brush has a distinctly higher temperature, which is due its function of conducting current. The summary of the steady state temperature of each component at all the speed ranges tested are shown in Table II.

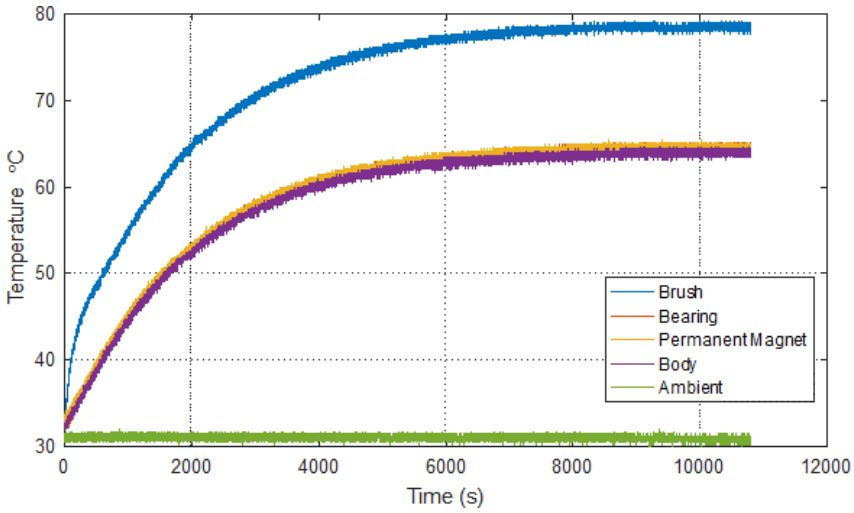

Figure 7. A sample of the temperature response data gathered at 40% of the nominal speed of 2650rpm.

Table 2. The steady state temperature (In ◦C) of all components at different speed.

Component	Speed (% of nominal speed of 2650rpm)				
	20%	40%	60%	80%	100%
Brush	71	79	85	79	70
Bearing	54	65	71	67	62
Perm. magnet	53	65	71	67	62
Casing	52	65	71	66	61

The temperature variation as the speed increase can be seen as in the graph in Figure 8. Rotating at higher speed generates higher temperatures across all components up until 60% of the nominal speed. After that, we observe a decreasing trend on the temprature.

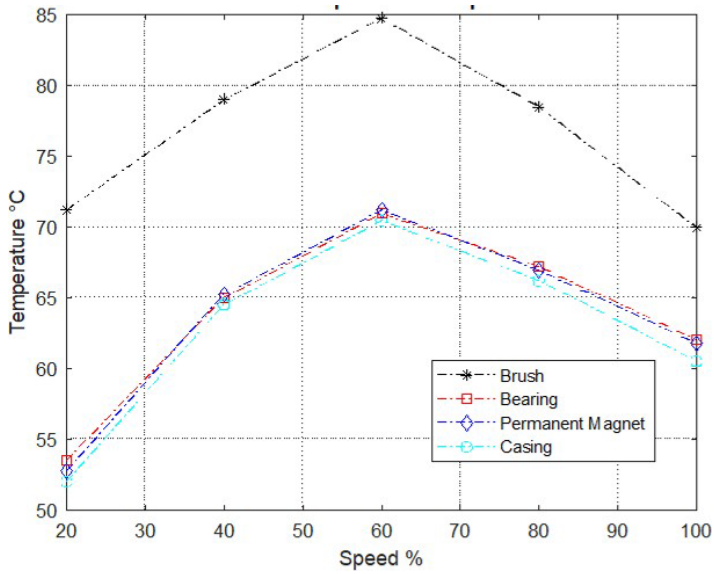

Figure 8. Steady state temperature of the MY1016 components at different speed.

Despite having the same negligible current of 4mA through the armature winding, the difference of temperatures exhibited at different speed suggest that the losses are different for each speed, and there is a phenomenon that could be explained as cooling at higher end speed. These differences in losses could not be originated from the copper losses, where the currents were shown to be the same. This could be explained by losses by frictions, especially mechanical due to bearing that increased with speed which is viscous in nature and proven to be non-negligible here. The temperature decrease at the end may potentially be due to air circulation in the machine that changes the convection rate. Therefore, the transfer function that will be developed will reflect the temperature variability due to this speed variability, but not current. We remind here that the objective is to develop a model that replicate the temperature response, without necessarily being able to physically explain the phenomenon, which will be a subject for a future study.

Transfer function identified

From the temperature response data above, the System Identification toolboxes deduce the transfer functions for each component and the error of each model. Table III below shows the resulting transfer function and the model error for the component brush. The brush being the most important component to be monitored, we are going to concentrate here on the brush first. The transfer function is certainly larger for a higher order, but that does not necessarily result in better precision. To better discern the trend of the model precision, Figure 9 below shows the MSE error plotted as a function of the number of poles of the model.

Table 3. The Identified Transfer Functions for Brush and its Corresponding Model Errors.

No. of Poles	Speed (%)	Transfer Function	MSE Error
1	20	$0.0002557\,/_{s+0.0003102}$	0.3202
	40	$0.0002454\,/s+0.0005232$	0.2475
	60	$0.0001781\,/_{s+0.0005156}$	0.6504
	80	$0.0001396\,/_{s+0.0006072}$	0.3042
	100	$8.05\text{e}\,5\,/_{s+0.00054}$	0.1794
2	20	$-6.06\text{e}-8/_{s^2+0.001757s+3.557\text{e}-14}$	113.9
	40	$4.607e-7/_{s^2+0.019s+1.38\text{e}-10}$	24.23
	60	$3.215\text{e}-7/_{s^2+\ 0.018s+7.99e-11}$	30.16
	80	$3.49e-7/_{s^2\ +0.029s+8.76e-\ 8}$	29.96
	100	$2.00e-7/_{s^2\ +0.025s+2.51e-9}$	17.91
3	20	$2.671e-9/_{s^3+0.00409s^2+1.184e-5s+3.223e-9}$	0.2366
	40	$4.19e-9/_{s^3+0.0048s^2+1.92e-5s+8.93e-9}$	0.1458
	60	$7.463e-9/_{s^3+0.0086s^2+4.73e-5s+2.15e-8}$	0.4134
	80	$1.86e-9/_{s^3+0.0081s^2+1.86e-5s+8.07e-9}$	0.2525
	100	$6.68e-10/_{s^3+0.0067s^2+1.20e-5s+4.47e-9}$	0.1533
4	20	$-1.9973-13/_{s^4+0.002s^3+7.22e-6s^2+9.24e-9s+2.11e-22}$	89.82
	40	$1.41e-12/_{s^4+0.011s^3+3.64e-5s^2+4.03s+2.20e-12}$	4.942
	60	$5.26e-13/_{s^4+0.0075s^3+1.79e-5s^2+1.82e-8s+1.17e-12}$	6.995
	80	$4.62e-13/_{s^4+0.0069s^3+1.93e-5s^2+1.75e-8s+1.78e-12}$	1.67
	100	$9.13e-4/_{s^4+0.0036s^3\ \ +4.89e-6s^2\ +1.35e-8s+7.94e-21}$	18.17

The first order has in general good model prediction with a maximum MSE error at 0.65 when the speed of the machine is at 60%. This is expected as we know that a temperature response is similar to a first order system. Despite could be taken as an overdamped system, the second order transfer function fails to model the temperature response together with the fourth order, having their MSE error values at an irrelevant value around 100. The surprise comes from the third order transfer function that shows an extremely good model prediction, at an even better precision then the first order at an MSE error of less than 0.41 across all speed.

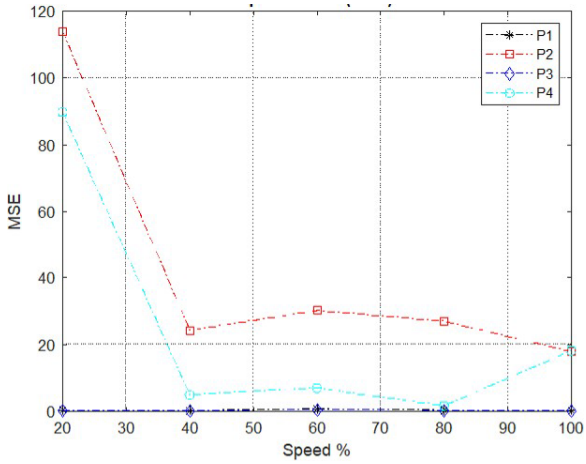

Figure 9. The model MSE error for the component brush at different choices of number of poles.

The third transfer function is then the transfer function of our choice, where it has the best precision across all speed. In comparison to the first order, the implementation of the third order transfer function would not generate any detectable additional computational cost. However, we can see from Table III that the transfer function identified at different speed (for the same poles = 3) are different. This shows that the heat transfer system across an electrical machine is not exactly an LTI system. This could be expected form the trend in the temperature variation previously observed on the experimental data (Fig. 8).

In a future follow-up study, the variation of the poles position across different speed will be scrutinized. This would lead to potentially researching an average transfer function that could be representative of the temperature response of the machine across its speed range.

CONCLUSION AND PERSPECTIVES

In this study, transfer functions were identified to model the temperature response inside the MY1016 dc machine at no load. It was found that the first and third order has sufficient precision to present the temperature response at a maximum MSE error of 0.65 and 0.41 respectively. The overdamped third order is the best model. The slight variation on the poles of the system indicate that the thermal system of the electrical machine does not obey exactly to the LTI hypothesis.

In a more complete transfer function model in the near future, this model would be added to a current input transfer function that would take into account the more prominent losses generated by the copper losses as the machine operates under load.

ACKNOWLEDGEMENTS

The authors would like to thank Universiti Malaysia Pahang for the facilities in the Electrical Drive System Laboratories and financial support by Yogyakarta State University through the 2022 International Cooperation Research between Universitas Negeri Yogyakarta and Universiti Malaysia Pahang (Agreement number: T/2.16/UN/34.21/PT.01.03/2022)

REFERENCES

[1] S. Nandi, H. A. Toliyat, and X. Li, “Condition Monitoring and Fault Diagnosis of Electrical Motors-A Review,” IEEE Transactions on Energy Conversion, vol. 20, pp. 719–729, 2005.

[2] J. E. Garcia-Bracamonte, J. M. Ramirez-Cortes, J. De, J. Rangel- Magdaleno, P. Gomez-Gil, H. Peregrina-Barreto, and V. Alarcon-Aquino, “An Approach on MCSA-Based Fault Detection Using Independent Component Analysis and Neural Networks,” IEEE Transactions on In- strumentation and Measurement, vol. 68, no. 5, pp. 1353–1361, 2019.

[3] Z. Meiwei, L. Weili, and T. Haoyue, “Demagnetization Fault Diagnosis of the Permanent Magnet Motor for Electric Vehicles Based on Tem- perature Characteristic Quantity,” IEEE Transactions on Transportation Electrification, vol. 9, pp. 759–770, 2023.

[4] S. Yilmaz and E. Ayaz, “Adaptive neuro-fuzzy inference system for bearing fault detection in induction motors using temperature, current, vibration data,” IEEE EUROCON, pp. 1140–1145, 2009.

[5] M. A. H. Rasid, M. N. A. Zulkafli, D. M. Nafiz, and N. F. Abdullah, “Experimental Evaluation of Temperature Distribution in Armature of a Brushed DC Machine Using Thermal Imaging,” in 2022 International Conference on Electrical Machines (ICEM), pp. 1927–1933.

[6] M. A. H. Rasid, A. Ospina, K. B. Benkara, and V. Lanfranchi, “A 3D Thermal Model of SynRM with Segmented Rotor Consider- ing Anisotropic Conductivity,” in 2021 IEEE 12th Energy Conversion Congress & Exposition - Asia (ECCE-Asia), 2021, pp. 1816–1822.

[7] B. Assaad, K. E. K. Benkara, S. Vivier, G. Friedrich, and A. Michon, “Thermal Design Optimization of Electric Machines Using a Global Sen- sitivity Analysis,” IEEE Transactions on Industry Applications, vol. 53, pp. 5365–5372, 2017.

[8] A. Pugachev and G. Fedyaeva, “Definition of the transfer function parameters of asynchronous motor as an object of temperature control,” Applied Mechanics and Materials, vol. 698, 2015..